

## Characterization of Ceria's Interaction with NO and NH

Li Zhang, John Pierce, Victor Leung, Di Wang, and William S. Epling

*J. Phys. Chem. C*, **Just Accepted Manuscript** • DOI: 10.1021/jp401442e • Publication Date (Web): 01 Apr 2013

Downloaded from <http://pubs.acs.org> on April 2, 2013

### Just Accepted

"Just Accepted" manuscripts have been peer-reviewed and accepted for publication. They are posted online prior to technical editing, formatting for publication and author proofing. The American Chemical Society provides "Just Accepted" as a free service to the research community to expedite the dissemination of scientific material as soon as possible after acceptance. "Just Accepted" manuscripts appear in full in PDF format accompanied by an HTML abstract. "Just Accepted" manuscripts have been fully peer reviewed, but should not be considered the official version of record. They are accessible to all readers and citable by the Digital Object Identifier (DOI®). "Just Accepted" is an optional service offered to authors. Therefore, the "Just Accepted" Web site may not include all articles that will be published in the journal. After a manuscript is technically edited and formatted, it will be removed from the "Just Accepted" Web site and published as an ASAP article. Note that technical editing may introduce minor changes to the manuscript text and/or graphics which could affect content, and all legal disclaimers and ethical guidelines that apply to the journal pertain. ACS cannot be held responsible for errors or consequences arising from the use of information contained in these "Just Accepted" manuscripts.



1  
2  
3  
4  
5  
6  
7  
8  
9  
10  
11  
12  
13  
14  
15  
16  
17  
18  
19  
20  
21  
22  
23  
24  
25  
26  
27  
28  
29  
30  
31  
32  
33  
34  
35  
36  
37  
38  
39  
40  
41  
42  
43  
44  
45  
46  
47  
48  
49  
50  
51  
52  
53  
54  
55  
56  
57  
58  
59  
60

# Characterization of Ceria's Interaction with $\text{NO}_x$ and $\text{NH}_3$

Li Zhang, John Pierce, Victor L. Leung, Di Wang and William S. Epling\*

Department of Chemical and Biomolecular Engineering, University of Houston

Houston, TX, 77204, USA

\*corresponding author

**ABSTRACT**

Ceria is a common component of engine aftertreatment catalysts, due to its oxygen storage ability, redox properties and its role in stabilizing Pt against sintering. In order to better understand the role of ceria in oxidation reactions occurring over a diesel oxidation catalyst (DOC), in the reduction of NO<sub>x</sub> on lean NO<sub>x</sub> traps (LNTs) and in the selective catalytic oxidation (SCO) of NH<sub>3</sub>, the interactions between ceria and NH<sub>3</sub> and/or NO<sub>x</sub> were investigated. Ceria proved active in NO oxidation, NH<sub>3</sub>-SCR and NH<sub>3</sub>-SCO reactions. Between 100-450°C, both NH<sub>3</sub> and NO<sub>x</sub> adsorbed on ceria simultaneously. In the absence of NO<sub>x</sub>, NH<sub>3</sub> was oxidized over CeO<sub>2</sub> forming N<sub>2</sub> via a two-step selective catalytic reduction mechanism at low temperature and NO<sub>x</sub> at high temperature. In the presence of NO<sub>x</sub>, NH<sub>3</sub> reacted with adsorbed NO<sub>x</sub> species, again forming N<sub>2</sub> at lower temperatures (250-450°C) while at higher temperature, a significant portion of the NH<sub>3</sub> was oxidized, with product NO formed.

**Keywords:** ceria; selective catalytic reduction; diesel oxidation catalyst; selective catalytic oxidation

## INTRODUCTION

Diesel engines are increasingly popular because of their better fuel economy, relative to gasoline engines, high torque output, resulting in their typical use as freight carriers, and durability. However, reducing some of the diesel engine exhaust emissions is challenging, with particulate matter (PM) and nitrogen oxide emissions receiving the most attention<sup>1,2</sup>. Currently, the diesel exhaust gas aftertreatment system is a combination of a diesel oxidation catalyst (DOC), a NO<sub>x</sub> storage/reduction (NSR or lean-NO<sub>x</sub> trap, LNT) catalyst and/or a selective catalytic reduction (SCR) catalyst, and a diesel particulate filter (DPF), to oxidize the CO and unburned hydrocarbons, reduce NO<sub>x</sub> and remove particulate matter<sup>3</sup>. In some cases, an NH<sub>3</sub> selective catalytic oxidation (SCO) catalyst is also used to minimize NH<sub>3</sub> slip resulting from overdosing urea<sup>4</sup>. In many aftertreatment system catalysts, ceria is added as part of the formulation due to its oxygen storage ability, redox properties and its role in stabilizing Pt against sintering<sup>5-16</sup>.

Typically, the DOC is positioned upstream of the other catalysts to oxidize the CO and unburned hydrocarbon emissions and to oxidize NO to NO<sub>2</sub>. Engine out ratios of NO<sub>2</sub>:NO are typically low and a higher ratio of NO<sub>2</sub>/NO increases the low temperature NO<sub>x</sub> conversion efficiency of SCR and NSR catalysts and NO<sub>2</sub> can oxidize soot at lower temperatures than O<sub>2</sub><sup>17-22</sup>. In terms of DPFs, recently it has been reported that ceria as a support results in interesting properties for soot combustion catalysts, due to a high availability of surface oxygen and good surface redox properties<sup>8,9,11-13</sup>.

In addition, CeO<sub>2</sub>-based SCR catalysts, such as ceria supported Pt, Pd and Rh, Cu/Ag/CeO<sub>2</sub>-ZrO<sub>2</sub>, CeO<sub>2</sub>-MnO<sub>x</sub>, Ce/TiO<sub>2</sub>, and Ce promoted Fe-exchanged TiO<sub>2</sub>-pillared clay<sup>5,23-29</sup> have been studied. It has been proposed that their NH<sub>3</sub>-SCR activities are at

1  
2  
3 least in part due to NO oxidation over, or associated with ceria<sup>26, 30</sup>. Also, a ceria-based  
4 catalyst has been studied for NH<sub>3</sub>-SCO<sup>31</sup>, providing high activity at low temperature due  
5 to its oxygen adsorption capacity. Many studies suggest that ceria promotes activity  
6 through its oxygen storage and redox properties, however, the published literature mainly  
7 focuses on the role of other catalytic materials, typically the precious metal components  
8 when studying DOCs and NSR catalysts, with the ceria playing a supporting role.  
9

10  
11  
12  
13  
14  
15  
16  
17  
18  
19  
20  
21  
22  
23  
24  
25  
26  
27  
28  
29  
30  
31  
32  
33  
34  
35  
36  
37  
38  
39  
40  
41  
42  
43  
44  
45  
46  
47  
48  
49  
50  
51  
52  
53  
54  
55  
56  
57  
58  
59  
60

NO<sub>x</sub> is a primary diesel engine pollutant and NH<sub>3</sub> is a reductant formed during NSR regeneration or added upstream of a SCR catalyst. Ceria is a common DOC and NSR catalyst component, and seems to be commonly added in new SCR formulations, thus it is important to understand the chemistry of NO<sub>x</sub> and NH<sub>3</sub> on ceria. In this study, the interactions between ceria and NO<sub>x</sub> and/or NH<sub>3</sub> were investigated using Diffuse Reflectance Infrared Fourier Transform Spectroscopy (DRIFTS) and reactor studies.

## EXPERIMENTAL METHODS

The ceria used in this study was purchased from Sigma Aldrich. The BET surface area was measured after degassing at 350 °C using a Gemini VII 2390 instrument. The surface area was found to be 5.2 m<sup>2</sup>/g.

The ceria particles were sieved to a particle size of 20-40 mesh and pretreated in a flow of 10% O<sub>2</sub>/N<sub>2</sub> at 500°C for 1 h or pretreated in a 20% H<sub>2</sub>/N<sub>2</sub> flow at 400°C for 1 h before testing. In the rest of this manuscript, the samples are labelled as fully oxidized ceria or reduced ceria, respectively, according to the pretreatment method.

NH<sub>3</sub>-SCR and NH<sub>3</sub>-SCO tests were carried out in a fixed bed reactor with 1.0 g of sample (20-40 mesh). The reaction gas mixture, using MKS mass flow controllers to set

1  
2  
3 the flow rates, for NH<sub>3</sub>-SCR consisted of 500 ppm NO, 500 ppm NH<sub>3</sub>, 10% O<sub>2</sub> and a N<sub>2</sub>  
4 balance. The total gas mixture flow rate was 200 cm<sup>3</sup>·min<sup>-1</sup>, resulting in a gas hourly  
5 space velocity (GHSV) of 18,000 h<sup>-1</sup>. The concentrations of NO, N<sub>2</sub>O, NO<sub>2</sub> and NH<sub>3</sub> were  
6 measured using a MKS MultiGas 2030 FTIR spectrometer. Similar reaction conditions  
7 were used for the NH<sub>3</sub>-SCO test, but NO was not included in the feed. NO oxidation was  
8 also carried out in the fixed bed reactor, where the reaction gas mixture consisted of 500  
9 ppm NO, 10% O<sub>2</sub> and a N<sub>2</sub> balance.

10  
11  
12  
13  
14  
15  
16  
17  
18  
19  
20 Reactions between NH<sub>3</sub> and the fully oxidized or reduced ceria (i.e. in the absence  
21 of gas-phase O<sub>2</sub>) were also studied in the fixed bed reactor. The experiment was carried  
22 out in a 500 ppm NH<sub>3</sub>/N<sub>2</sub> flow at 350, 400 and 450°C in the absence of gas-phase O<sub>2</sub>.  
23 Effluent gaseous NO, NO<sub>2</sub> and N<sub>2</sub>O concentrations were monitored. NO interactions with  
24 the fully oxidized or reduced ceria were also monitored in the fixed bed reactor under  
25 similar conditions. Separate experiments were performed in order to quantify the surface  
26 oxygen available for reaction with NO and the formation of surface nitrates on ceria. The  
27 experiments were performed in a 125 ppm NO and balance N<sub>2</sub> flow over 1.0 g of fully  
28 oxidized ceria. The available/reactive oxygen was calculated by measuring the difference  
29 of the known inlet concentration of NO from the amount of NO detected during the  
30 reaction and assuming that was used for NO<sub>2</sub> and nitrate formation. The measurement  
31 ended when the outlet value reached within 2% of the inlet concentration value.

32  
33  
34  
35  
36  
37  
38  
39  
40  
41  
42  
43  
44  
45  
46  
47  
48 Surface species formed during exposure of the ceria to NO and NH<sub>3</sub> were  
49 characterized with in-situ Diffuse Reflectance Infrared Fourier Transform Spectroscopy  
50 (DRIFTS). A Nicolet 6700 FT-IR spectrometer equipped with a Harrick Scientific  
51 DRIFTS cell and a mercury-cadmium-telluride (MCT) detector was used. 200 mg of  
52  
53  
54  
55  
56  
57  
58  
59  
60

1  
2  
3 sample was placed in a ceramic crucible. A feed gas mixture, controlled using MKS mass  
4 flow controllers, was supplied at a flow rate of  $50 \text{ cm}^3 \cdot \text{min}^{-1}$ . The samples were first  
5  
6 treated in a flow of 10%  $\text{O}_2/\text{He}$  at  $500^\circ\text{C}$  for 0.5 h and then cooled to room temperature.  
7  
8 For the experiments characterizing the reduced surface, the sample was exposed to a  $\text{H}_2$ -  
9  
10 pretreatment in a flow of 20%  $\text{H}_2/\text{He}$  at  $400^\circ\text{C}$  for 1 h before being cooled to the desired  
11  
12 temperature in a flow of He. At the temperatures used for analysis, a background  
13  
14 spectrum was recorded in flowing He, and it was subtracted from the sample spectrum  
15  
16 obtained at the same temperature. The DRIFTS spectra were collected from 4000 to 650  
17  
18  $\text{cm}^{-1}$ , accumulating 100 scans at a  $4 \text{ cm}^{-1}$  resolution. Nicolet OMNIC software was used  
19  
20 to convert the absorbance data into Kubelka-Munk (KM) format.  
21  
22  
23  
24  
25  
26

27 Note, water was not included in these studies although admittedly it could have an  
28  
29 impact on the relative amounts of adsorbed species observed upon exposure to  $\text{NH}_3$   
30  
31 and/or  $\text{NO}_x$ . However, to being to gain a fundamental understanding of ceria's  
32  
33 interactions with these species, water was excluded in order to simplify the analysis.  
34  
35 Future work will include its impact.  
36  
37  
38  
39  
40

## 41 **RESULTS AND DISCUSSION**

### 42 *$\text{NH}_3$ -SCR and $\text{NH}_3$ -SCO*

43  
44  
45 The conversion results as a function of temperature obtained during  $\text{NH}_3$ -SCR of  
46  
47 NO over the fully oxidized ceria sample are shown in Figure 1. Appreciable  $\text{NH}_3$ -SCR  
48  
49 activity was observed between  $270$ - $420^\circ\text{C}$ . The activity data for selective catalytic  
50  
51 oxidation of  $\text{NH}_3$  over ceria and product selectivity are shown in Figure 2. Between  $300$ -  
52  
53  $450^\circ\text{C}$ ,  $\text{NH}_3$  was oxidized to mainly  $\text{N}_2$ ; while at higher temperature, the main product  
54  
55  
56  
57  
58  
59  
60

1  
2  
3 was NO. With N<sub>2</sub> as the product, it is likely that the NH<sub>3</sub> is oxidized to NO, and then  
4  
5  
6 SCR occurs over the surface, since as shown in Figure 1, within this temperature range  
7  
8 the SCR reaction readily occurs. A very small amount of N<sub>2</sub>O was formed in the 400°C  
9  
10 range. These results also demonstrate that above 400°C, the SCR activity dropped due to  
11  
12 NH<sub>3</sub> oxidation leading to NO as a product. Thus there is not only the loss of the reductant  
13  
14 but also formation of more NO.  
15  
16

17  
18 The interaction of NH<sub>3</sub> with ceria's surface oxygen was studied by exposing the  
19  
20 ceria to an NH<sub>3</sub>/N<sub>2</sub> mixture in the absence of gas-phase O<sub>2</sub>. NH<sub>3</sub>, NO and N<sub>2</sub>O  
21  
22 concentrations as a function of time are shown in Figure 3. In this absence of gaseous O<sub>2</sub>,  
23  
24 no NO<sub>2</sub> was detected. With increasing temperature, there was increasing NH<sub>3</sub>  
25  
26 consumption or adsorption, as shown in Figure 3a. During the approach to the inlet  
27  
28 concentration, NH<sub>3</sub> was oxidized to both NO and N<sub>2</sub>O, Figure 3b and c, respectively. The  
29  
30 NO and N<sub>2</sub>O product concentrations increased as a function of time, and then decreased,  
31  
32 with the rate of decrease higher with increasing temperature. NH<sub>3</sub> was oxidized by the  
33  
34 stored oxygen on ceria and as oxygen was consumed the NO and N<sub>2</sub>O concentrations  
35  
36 dropped, indicating a limited supply of oxygen was available. The consumed NH<sub>3</sub>, and  
37  
38 NO and N<sub>2</sub>O formed, were quantified and are listed in Table 1. A significant amount of  
39  
40 N<sub>2</sub> was produced in this reaction, as indicated in Figure 2b, resulting in the imbalance  
41  
42 noted. Furthermore, surface N species formed, as will be discussed below. As  
43  
44 temperature increased, more NH<sub>3</sub> was consumed but more NO was formed, which is  
45  
46 consistent with the results obtained in the presence of gas-phase O<sub>2</sub> (Figure 2).  
47  
48  
49  
50  
51  
52  
53  
54  
55  
56  
57  
58  
59  
60

1  
2  
3 A similar experiment (results not shown), involving the interaction between  $\text{NH}_3$   
4 and reduced ceria, showed no  $\text{NH}_3$  oxidation, indicating that the reduction process  
5 removed any reactive surface oxygen.  
6  
7  
8  
9

### 10 11 12 *NO oxidation*

13  
14  
15 Many studies have shown that if a zeolite-based SCR catalyst can oxidize NO to  
16  $\text{NO}_2$  in-situ, its low temperature SCR activity will be significantly enhanced, as the  
17 presence of  $\text{NO}_2$  allows the “fast SCR” reaction to proceed<sup>21, 22</sup>. In addition, if a DOC  
18 catalyst is active in NO oxidation to  $\text{NO}_2$ , this can lead to a decrease in the temperature  
19 required for soot oxidation on a DPF<sup>12, 19, 20, 32, 33</sup>. NO oxidation conversion as a function  
20 of temperature over oxidized ceria results are shown in Figure 4. NO oxidation was  
21 observed above 200°C and increased with temperature to around 400°C, and then  
22 decreased with increasing temperature, due to thermodynamic equilibrium limitations.  
23  
24  
25  
26  
27  
28  
29  
30  
31  
32  
33

34 To further investigate NO oxidation over ceria, the interaction of NO with stored  
35 surface oxygen was studied. Fully oxidized ceria was exposed to 500 ppm NO/ $\text{N}_2$  at 350,  
36 400 and 450°C and the NO and  $\text{NO}_2$  concentration profiles as a function of time are  
37 shown in Figure 5. NO was oxidized to  $\text{NO}_2$ , with the most formed at 400°C, which is  
38 consistent with the results shown in Figure 4. In the presence of gaseous  $\text{O}_2$ , more  $\text{NO}_2$   
39 was formed as would be expected with ever diminishing oxygen reactant as a function of  
40 time in its absence. The higher NO oxidation activity at 400°C coincides with the best  
41 SCR of NO conversion being attained, suggesting that SCR of  $\text{NO}_2$  proceeds at a faster  
42 rate than NO SCR or that  $\text{NO}_2$  is a required intermediate, as has been proposed in  
43 previous studies<sup>29, 34, 35</sup>. Additionally, the same experiment was performed with reduced  
44  
45  
46  
47  
48  
49  
50  
51  
52  
53  
54  
55  
56  
57  
58  
59  
60

1  
2  
3 ceria, however, NO<sub>2</sub> was not detected (results not shown). This result, similar to that  
4  
5 obtained with NH<sub>3</sub> exposure to the reduced ceria surface, further confirms that the stored  
6  
7 surface oxygen on ceria can play a role in NO oxidation.  
8  
9

10 The amount of surface oxygen that reacted with NO, and the formed nitrates  
11  
12 adsorbed on ceria, at various temperatures were quantified and the results are listed in  
13  
14 Table 2. Although other surface NO<sub>x</sub> species formed, verified via DRIFTS as will be  
15  
16 discussed below, nitrate formation was dominant and is assumed for quantification  
17  
18 comparison. Adsorption was observed in the entire temperature range examined and with  
19  
20 little NO<sub>2</sub> produced, most resulted in nitrate formation. At lower temperatures, more  
21  
22 surface NO<sub>x</sub> species formed, suggesting a higher level of oxygen availability, compared  
23  
24 to that at higher temperatures. This is somewhat surprising as typically oxygen mobility  
25  
26 would increase with increasing temperature and the results shown in Figure 5  
27  
28 demonstrate NO<sub>2</sub> formation increased at least from 350 to 400°C. The consumption trend  
29  
30 is instead due to nitrate stability, with the surface NO<sub>x</sub> species decomposing and NO  
31  
32 release occurring with increasing temperature, thus the lower levels measured. The total  
33  
34 available oxygen, assuming CeO<sub>2</sub>, had a maximum utilized at 100°C, and was 17% of the  
35  
36 total available oxygen in the ceria sample.  
37  
38  
39  
40  
41  
42  
43  
44

#### 45 *NH<sub>3</sub> adsorption*

46  
47  
48 DRIFTS was used to characterize the surface species formed during NH<sub>3</sub>  
49  
50 adsorption on ceria. The DRIFTS spectra obtained during exposure of the fully oxidized  
51  
52 and reduced ceria samples to NH<sub>3</sub> at various temperatures are shown in Figure 6. During  
53  
54 exposure of the fully oxidized sample at room temperature, bands at 1676, 1433 and 1394  
55  
56  
57  
58  
59  
60

1  
2  
3  $\text{cm}^{-1}$  appeared and are assigned to Brønsted acid sites, i.e.  $\text{NH}_4^+$  on  $\text{CeO}_2$ <sup>6, 31</sup>. The  
4  
5 features at 1570, 1286 and 1147  $\text{cm}^{-1}$  are attributed to  $\text{NH}_3$  coordinated to Lewis acid  
6  
7 sites<sup>6, 36</sup> and at 1556 and 1261  $\text{cm}^{-1}$  are assigned to amide species ( $-\text{NH}_2$ )<sup>36-38</sup>. The  $\text{NH}_3$   
8  
9 coordinated Brønsted acid site and Lewis acid site features were less intense with  
10  
11 increasing exposure temperature. However,  $\text{NH}_3$  adsorbed on Brønsted acid sites  
12  
13 disappeared at a lower temperature, indicating that  $\text{NH}_3$  was more stable on the Lewis  
14  
15 acid sites. In addition, the amide species bands (1556 and 1261  $\text{cm}^{-1}$ ) evident with room  
16  
17 temperature exposure, increased in intensity with temperature and then decreased in  
18  
19 intensity at higher temperatures ( $>400^\circ\text{C}$ ). These results indicate that upon heating, some  
20  
21 adsorbed  $\text{NH}_3$  on ceria formed  $-\text{NH}_2$  through abstraction of hydrogen likely in reducing  
22  
23 the ceria.  
24  
25  
26  
27  
28

29  
30 With increasing temperature, specifically in the 300-400 $^\circ\text{C}$  range, new bands at  
31  
32 1545, 1371, 1358 and 1305  $\text{cm}^{-1}$  appeared, which are assigned to surface  $\text{NO}_x$  species. At  
33  
34 temperatures above 400 $^\circ\text{C}$ , these bands disappeared and four new features (1560, 1523,  
35  
36 1276 and 1220  $\text{cm}^{-1}$ ), also associated with adsorbed  $\text{NO}_x$ , appeared. Based on previous  
37  
38 studies, these peaks are tentatively assigned to adsorbed monodentate (1523 and 1276  $\text{cm}^{-1}$   
39  
40 <sup>1</sup>), bidentate (1545 and 1305  $\text{cm}^{-1}$ ) and bridging nitrate species (1560 and 1220  $\text{cm}^{-1}$ )<sup>6, 26,</sup>  
41  
42 <sup>36, 39-41</sup>. The assignment of the bands at 1371 and 1358  $\text{cm}^{-1}$  is discussed in more detail  
43  
44 below. According to the results shown in Figure 3, no  $\text{NO}_2$  was formed during  $\text{NH}_3$   
45  
46 oxidation in the absence of gas-phase  $\text{O}_2$ . As a result, the observed  $\text{NO}_x$  ad-species must  
47  
48 be a result of  $\text{NO}$  formation via  $\text{NH}_3$  oxidation with the participation of ceria surface or  
49  
50 lattice oxygen, and further oxidation of this surface species via the available surface  
51  
52 oxygen.  
53  
54  
55  
56  
57  
58  
59  
60

1  
2  
3 To further investigate the role of the surface or lattice oxygen on NH<sub>3</sub> adsorption,  
4  
5 a similar experiment was performed on the reduced ceria sample (H<sub>2</sub> pre-treatment at  
6  
7 400°C). Bands associated with Bronsted acid sites (1676, 1516, 1433 and 1394 cm<sup>-1</sup>) and  
8  
9 Lewis acid sites (1570, 1286 and 1147 cm<sup>-1</sup>) were again observed following NH<sub>3</sub>  
10  
11 adsorption (Figure 6(b)). These bands disappeared at a lower temperature (250°C)  
12  
13 relative to those on the oxidized sample. In addition, all adsorbed NH<sub>3</sub> band intensities on  
14  
15 reduced ceria were lower than those on fully oxidized ceria, demonstrating that less NH<sub>3</sub>  
16  
17 adsorbed and the NH<sub>3</sub> that did adsorb was more weakly bound to the reduced ceria  
18  
19 surface. While the intensity of these bands decreased with increasing temperature, bands  
20  
21 corresponding to -NH<sub>2</sub> (1556 and 1261 cm<sup>-1</sup>)<sup>36-38</sup> again were evident at room temperature,  
22  
23 but simply decreased with increasing temperature. No new bands associated with NO<sub>x</sub> ad-  
24  
25 species were observed, which indicates that the NH<sub>3</sub> that adsorbed and further reacted on  
26  
27 the reduced ceria mainly formed -NH<sub>2</sub> and was not oxidized to NO. This is consistent  
28  
29 with reactor experiments that showed no NH<sub>3</sub> oxidation as mentioned above.  
30  
31  
32  
33  
34  
35  
36  
37  
38

### 39 *NO<sub>x</sub> adsorption*

40  
41 DRIFTS spectra obtained during adsorption of NO, in the absence of gas phase O<sub>2</sub>,  
42  
43 on the fully oxidized and reduced ceria samples at different temperatures are shown in  
44  
45 Figure 7. Based on literature studies, the peaks in Figure 7(a), obtained with the fully  
46  
47 oxidized sample, are tentatively assigned to adsorbed bidentate (1575 and 1305 cm<sup>-1</sup>),  
48  
49 monodentate (1535 and 1276 cm<sup>-1</sup>), water-solvated (1485 cm<sup>-1</sup>), and bridging (1608 and  
50  
51 1230 cm<sup>-1</sup>) nitrate species<sup>6, 26, 36, 39-41</sup>. The band at 1442 cm<sup>-1</sup> is assigned to *trans*-N<sub>2</sub>O<sub>2</sub><sup>2-26,</sup>  
52  
53  
54  
55  
56  
57  
58  
59  
60  
42. With increasing temperature, the bridging, monodentate and bidentate nitrate species'

1  
2  
3 concentrations gradually decreased. In addition, bands that appeared at 1371 and 1358  
4  
5  $\text{cm}^{-1}$  show similar trends, which are close to the reported *cis*- $\text{N}_2\text{O}_2^{2-}$  band ( $1350 \text{ cm}^{-1}$ ) of  
6  
7  $\text{NO}_x$  adsorption on pure ceria <sup>26</sup>.  
8  
9

10  
11 According to the results obtained during  $\text{NH}_3$  adsorption (Figure 6 (a)) on the  
12  
13 oxidized ceria sample, the bands assigned to  $\text{NO}_x$  ad-species appeared in similar regions  
14  
15 as those associated with the  $\text{NO}_x$  ad-species during the  $\text{NO}$  exposure experiment, which  
16  
17 demonstrates that in the presence of surface oxygen, adsorbed  $\text{NH}_3$  was indeed oxidized  
18  
19 to form intermediate surface  $\text{NO}_x$  species at higher temperature.  
20  
21

22  
23 The DRIFTS spectra obtained during  $\text{NO}$  adsorption on the reduced ceria are  
24  
25 shown in Figure 7 (b), with significant differences observed compared to those obtained  
26  
27 from the fully oxidized ceria. Features at 1608 (bridging nitrates), 1442, 1385 (*trans*-  
28  
29  $\text{N}_2\text{O}_2^{2-}$ ), 1371, 1358 (*cis*- $\text{N}_2\text{O}_2^{2-}$ ), 1575, 1305 (bidentate nitrates), 1535, 1276  
30  
31 (monodentate nitrates), and  $1176 \text{ cm}^{-1}$  were evident at room temperature. With increasing  
32  
33 temperature ( $>100 \text{ }^\circ\text{C}$ ), the adsorbed bidentate nitrates vanished, and the bridging and  
34  
35 monodentate nitrate bands shifted to lower wavenumbers ( $1558, 1230 \text{ cm}^{-1}$  and  $1523,$   
36  
37  $1276 \text{ cm}^{-1}$ ) due to the lower coverage. The band at  $1176 \text{ cm}^{-1}$  can be assigned to  $\text{NO}^-$  ad-  
38  
39 species ( $1180 \text{ cm}^{-1}$ ) on ceria <sup>26</sup>. The  $\text{NO}$  adsorption bands on reduced ceria were of lower  
40  
41 intensity and thermal stability than those of the oxidized sample, thus the stored surface  
42  
43 oxygen promoted  $\text{NO}$  adsorption as would be expected.  
44  
45  
46  
47

48  
49 With available/reactive oxygen,  $\text{NO}$  reacted with stored surface oxygen to form  
50  
51  $\text{NO}_2$  and surface nitrates. Previous literature density functional theory calculation results  
52  
53 indicate that Ce (III) could be oxidized by  $\text{NO}_2$  to form Ce (IV) <sup>43</sup>. However,  
54  
55 experimental evidence regarding whether  $\text{NO}_2$  could oxidize ceria and how it interacts  
56  
57  
58  
59  
60

1  
2  
3 with the ceria has not been reported. To characterize this interaction, DRIFTS spectra of  
4  
5  
6 NO<sub>2</sub> adsorption on reduced ceria at various temperatures were obtained. As shown in  
7  
8 Figure 8, similar species as those noted in Figure 7(a), bridging nitrates (1608 and 1230  
9  
10 cm<sup>-1</sup>), bidentate nitrates (1575 and 1305 cm<sup>-1</sup>), monodentate nitrates (1535 and 1276 cm<sup>-1</sup>)  
11  
12 <sup>1</sup>), water solvated nitrates (1485 cm<sup>-1</sup>), *trans*-N<sub>2</sub>O<sub>2</sub> (1442 cm<sup>-1</sup>) and *cis*-N<sub>2</sub>O<sub>2</sub> (1371 and  
13  
14 1358 cm<sup>-1</sup>), were observed. The band intensities during NO<sub>2</sub> adsorption were larger in  
15  
16 comparison to those associated with the fully oxidized or reduced ceria exposure to NO  
17  
18 exposure (Figure 7), indicating more significant nitrate formation with NO<sub>2</sub> as the inlet  
19  
20 NO<sub>x</sub> species. Based on the results obtained during NO interaction with reduced ceria  
21  
22 (Figure 5), no NO<sub>2</sub> formed. For NO interaction with the fully oxidized ceria, the band at  
23  
24 1176 cm<sup>-1</sup>, NO<sup>-</sup>, was absent, which indicates that adsorbed NO was oxidized to form NO<sub>2</sub>,  
25  
26 or more highly oxidized surface species by the stored surface oxygen. In addition, bands  
27  
28 at 1371 and 1358 cm<sup>-1</sup>, due to the N<sub>2</sub>O<sub>2</sub><sup>2-</sup> ad-species, were evident in Figure 8, likely due  
29  
30 to NO<sub>2</sub> oxidizing the reduced ceria and NO dimerization then following. These combined  
31  
32 results all indicate that a larger extent of NO<sub>x</sub> adsorption on fully oxidized ceria can be  
33  
34 realized with NO<sub>2</sub> formation or availability.  
35  
36  
37  
38  
39  
40  
41  
42

#### 43 44 *Reaction between NH<sub>3</sub> and O<sub>2</sub>*

45  
46 The interaction of NH<sub>3</sub> and ceria in the presence of gaseous O<sub>2</sub> was also studied  
47  
48 with results shown in Figure 9. The bands attributed to NH<sub>3</sub> coordinated on Brønsted acid  
49  
50 sites (1676, 1433 and 1394 cm<sup>-1</sup>), Lewis acid sites (1570, 1286 and 1147 cm<sup>-1</sup>) and -NH<sub>2</sub>  
51  
52 (1261cm<sup>-1</sup>) decreased gradually with temperature and were absent at temperatures higher  
53  
54 than 350°C, similar to the trends observed in the absence of gas-phase O<sub>2</sub>. While these  
55  
56  
57  
58  
59  
60

1  
2  
3 band intensities decreased, features appeared at 1545, 1305 (bidentate nitrates), 1358 and  
4  
5  
6  $1371\text{ cm}^{-1}$  (*cis*- $\text{N}_2\text{O}_2^{2-}$ ) at temperatures above  $300^\circ\text{C}$  and disappeared at temperatures  
7  
8 above  $400^\circ\text{C}$ . Above  $400^\circ\text{C}$ , several new bands appeared; at 1523, 1276 (monodentate  
9  
10 nitrates), 1558, 1220 (bridging nitrates) and  $1176\text{ cm}^{-1}$  ( $\text{NO}^-$ ). These spectra demonstrate  
11  
12 that  $\text{NH}_3$  was oxidized to form NO at temperatures higher than  $300^\circ\text{C}$ , and the formed  
13  
14 adsorbed NO was further oxidized to bidentate nitrates ( $1545$  and  $1305\text{ cm}^{-1}$ ) between  
15  
16  $300$ - $400^\circ\text{C}$ . At higher temperature ( $>400^\circ\text{C}$ ), the surface NO mainly formed monodentate  
17  
18 nitrate ( $1523$  and  $1276\text{ cm}^{-1}$ ), bridging nitrate ( $1558$ ,  $1220\text{ cm}^{-1}$ ) and  $\text{NO}^-$  ( $1176\text{ cm}^{-1}$ )  
19  
20 species. The same trends were noted in Figure 6a, indicating the stability of these species  
21  
22 and the surface reactions were surprisingly not influenced by gas-phase  $\text{O}_2$ .  
23  
24  
25  
26  
27  
28  
29

### 30 *Reaction between $\text{NH}_3$ and $\text{NO}_x$*

31  
32 The interaction between  $\text{NH}_3$ , NO and  $\text{O}_2$  on ceria was also investigated (Figure  
33  
34 9(b)). Features assigned to  $\text{NH}_3$  coordinated on Brønsted acid sites ( $1676$ ,  $1516$ ,  $1433$  and  
35  
36  $1394\text{ cm}^{-1}$ ), Lewis acid sites ( $1286\text{ cm}^{-1}$ ) and  $-\text{NH}_2$  ( $1261\text{ cm}^{-1}$ ) species were detected at  
37  
38 lower temperatures ( $<200^\circ\text{C}$ ). A  $\text{NO}^-$  band ( $1176\text{ cm}^{-1}$ ) appeared at  $100^\circ\text{C}$  and decreased  
39  
40 with increasing temperature, while bands assigned to other  $\text{NO}_x$  ad-species ( $1545$ ,  $1371$ ,  
41  
42  $1358$  and  $1305\text{ cm}^{-1}$ ) appeared at  $<200^\circ\text{C}$ , increased significantly as temperature  
43  
44 increased, and then decreased at temperatures above  $450^\circ\text{C}$ . According to the results  
45  
46 shown in Figure 9 (a), some  $\text{NO}_x$  ad-species ( $1545$ ,  $1371$ ,  $1358$  and  $1305\text{ cm}^{-1}$ ) appeared  
47  
48 only between  $250$ - $350^\circ\text{C}$ , and adsorbed  $\text{NO}^-$  ( $1176\text{ cm}^{-1}$ ) appeared at temperatures higher  
49  
50 than  $400^\circ\text{C}$  during  $\text{NH}_3$  oxidation, which indicates that the same peaks appearing at low  
51  
52 temperature ( $<200^\circ\text{C}$ ) in Figure 9 (b) were not due to  $\text{NH}_3$  oxidation, but specifically to  
53  
54  
55  
56  
57  
58  
59  
60

1  
2  
3 NO<sub>x</sub> adsorption. Combined with the results of NH<sub>3</sub>-SCR shown in Figure 1, NH<sub>3</sub> reacted  
4  
5 with the NO to form N<sub>2</sub> below 350°C, further confirming these DRIFTS features are due  
6  
7 to NO adsorption. These spectra show that ceria can adsorb NH<sub>3</sub> and NO<sub>x</sub> simultaneously  
8  
9 between 100-450°C.  
10  
11

12  
13 Separate experiments were run with pre-adsorbed NO<sub>x</sub>. As noted already, NO  
14  
15 coordinated species (1560, 1535, 1371, 1358, 1280 and 1232 cm<sup>-1</sup>) formed on ceria upon  
16  
17 exposure to NO (Figure 10(a)). With exposure to NH<sub>3</sub> at 350°C, the NO<sub>x</sub> species  
18  
19 adsorbed at 1371, and 1358 cm<sup>-1</sup> decreased gradually and then disappeared, which  
20  
21 indicates that NH<sub>3</sub> reacted with the adsorbed NO<sub>x</sub>. However, the intensity of the bands at  
22  
23 1560 and 1232 (bridging nitrates) decreased slightly, and the features at 1280 and 1535  
24  
25 cm<sup>-1</sup>, assigned to monodentate nitrate species, did not decrease. Therefore, we conclude  
26  
27 that NO<sub>x</sub> adsorbed as *cis*-N<sub>2</sub>O<sub>2</sub><sup>2-</sup> reacted more favorably with NH<sub>3</sub> than other nitrates ad  
28  
29 species. The lack of any new features appearing demonstrates that NH<sub>3</sub> readily reacted  
30  
31 with the adsorbed NO at 350°C.  
32  
33  
34  
35

36  
37 These results suggest a reaction route for NH<sub>3</sub> oxidation. NO<sub>x</sub> ad species (1371  
38  
39 and 1358 cm<sup>-1</sup>) were observed during NH<sub>3</sub> oxidation between 300-350°C (Figure 9 (a)).  
40  
41 In addition, the results in Figure 10(a) demonstrate that the same surface NO<sub>x</sub> species  
42  
43 (*cis*-N<sub>2</sub>O<sub>2</sub><sup>2-</sup> at 1371 and 1358 cm<sup>-1</sup>) reacted with NH<sub>3</sub>, suggesting that the NO species  
44  
45 formed during NH<sub>3</sub> oxidation reacted with the NH<sub>3</sub> to form N<sub>2</sub>. NH<sub>3</sub> oxidation over ceria  
46  
47 thus follows a two-step SCR mechanism; some NH<sub>3</sub> is oxidized to form NO, which then  
48  
49 reacts with the NH<sub>3</sub> to form N<sub>2</sub>. At temperatures above 400°C (Figure 9 (a)), this  
50  
51 intermediate NO<sub>x</sub> surface species was absent, with other surface NO<sub>x</sub> species observed:  
52  
53 monodentate nitrates (1523 and 1276 cm<sup>-1</sup>), bridging nitrates (1558 and 1220 cm<sup>-1</sup>) and  
54  
55  
56  
57  
58  
59  
60

1  
2  
3 NO<sup>-</sup> (1176 cm<sup>-1</sup>), which are apparently not reactive with the NH<sub>3</sub>, or NH<sub>3</sub> is too quickly  
4 oxidized to higher oxidation states, but they do decompose to form gas-phase NO. This  
5 conclusion is consistent with the reactor results (Figure 2).  
6  
7

8  
9  
10 Ceria can catalyze NO oxidation (Figure 4) and thus the surface species formed  
11 via NO<sub>2</sub> adsorption can also react with NH<sub>3</sub>; the DRIFTS results obtained during NH<sub>3</sub>  
12 exposure after a pre-exposure to NO<sub>2</sub> are shown in Figure 10 (b). Features were evident  
13 at 1594 and 1207 cm<sup>-1</sup> (weakly adsorbed NO<sub>2</sub>),<sup>26</sup> and the other features had stronger  
14 intensities compared to those obtained during NO adsorption at 350°C (Figure 10 (a)).  
15 With the addition of NH<sub>3</sub>, the adsorbed NO<sub>2</sub> (1594 and 1207 cm<sup>-1</sup>) and *vis*-N<sub>2</sub>O<sub>2</sub><sup>2-</sup> (1371  
16 and 1358 cm<sup>-1</sup>), decreased gradually. Also, the bidentate, monodentate and bridging  
17 nitrate species were again not reactive with the NH<sub>3</sub>.  
18  
19  
20  
21  
22  
23  
24  
25  
26  
27  
28  
29  
30  
31

## 32 CONCLUSIONS

33  
34 Ceria readily adsorbs NH<sub>3</sub> and NO<sub>x</sub>. The adsorbed NH<sub>3</sub> can be oxidized by ceria's surface  
35 oxygen at higher temperatures, forming surface NO<sub>x</sub> species, and the NH<sub>3</sub> and surface  
36 NO<sub>x</sub> species can in turn react to form N<sub>2</sub>. Upon NO<sub>x</sub> exposure, NO<sub>x</sub> adsorption on ceria  
37 was observed in the entire temperature range evaluated (30-500°C). At lower  
38 temperatures, more NO<sub>x</sub> adsorbed or surface NO<sub>x</sub> species formed, due to surface ad-  
39 species stability, i.e. formed nitrates decomposed at higher temperatures. NH<sub>3</sub> and NO<sub>x</sub>  
40 can adsorb on the ceria simultaneously, also leading to some SCR, but only certain  
41 surface NO<sub>x</sub> species participate. Furthermore, the stored surface oxygen on ceria induces  
42 more significant NH<sub>3</sub> and NO<sub>x</sub> adsorption.  
43  
44  
45  
46  
47  
48  
49  
50  
51  
52  
53  
54  
55  
56  
57  
58  
59  
60

**REFERENCES**

1. Johnson, T. V. Diesel Emission Control in Review -The Last 12 Months. *SAE Technical Paper Series*. **2003**, 2003-01-0039.
2. Charlton, S. J. Developing Diesel Engines to Meet Ultra-low Emission Standards. *SAE Technical Paper Series*. **2005**, 2005-01-3628.
3. Gurupatham, A.; He, Y. Architecture Design and Analysis of Diesel Engine Exhaust Aftertreatment System and Comparative Study with Close-coupled DOC-DPF System. *SAE Int. J. Fuels Lubr.* **2008**, *1*, 1387-1396.
4. Girard, J. W.; Cavataio, G.; Lambert, C. K. The Influence of Ammonia Slip Catalysts on Ammonia, N<sub>2</sub>O and NO<sub>x</sub> Emissions for Diesel Engines. *SAE Technical Paper Series*. **2007**, 2007-01-1572.
5. Chen, L.; Li, J.; Ge, M.; Zhu, R. Enhanced activity of tungsten modified CeO<sub>2</sub>/TiO<sub>2</sub> for selective catalytic reduction of NO<sub>x</sub> with ammonia. *Catal.Today*. **2010**, *153*, 77-83.
6. Shan, W.; Liu, F.; He, H.; Shi, X.; Zhang, C. Novel cerium-tungsten mixed oxide catalyst for the selective catalytic reduction of NO<sub>x</sub> with NH<sub>3</sub>. *Chem. Comm.* **2011**, *47*, 8046-8048.
7. Si, Z.; Weng, D.; Wu, X.; Ran, R.; Ma, Z. NH<sub>3</sub>-SCR activity, hydrothermal stability, sulfur resistance and regeneration of Ce<sub>0.75</sub>Zr<sub>0.25</sub>O<sup>2</sup>-PO<sub>4</sub><sup>3-</sup>-catalyst. *Catal. Comm.* **2012**, *17*, 146-149.
8. Fang, P.; Lu, J.; Xiao, X.; Luo, M. Catalytic combustion study of soot on Ce<sub>0.7</sub>Zr<sub>0.3</sub>O<sub>2</sub> solid solution. *J.Rare Earths*. **2008**, *26*, 250-253.
9. Guillén-Hurtado, N.; Bueno-López, A. ; García-García, A. Catalytic performances of ceria and ceria-zirconia materials for the combustion of diesel soot under NO<sub>x</sub>/O<sub>2</sub> and O<sub>2</sub>. Importance of the cerium precursor salt. *Appl. Catal. A*. **2012**, *437*, 166-172.
10. Kašpar, J.; Fornasiero, P.; Graziani, M. Use of CeO<sub>2</sub>-based oxides in the three-way catalysis. *Catal.Today*. **1999**, *50*, 285-298.

- 1  
2  
3 11. Weng, D.; Li, J.; Wu, X.; Si, Z. Modification of CeO<sub>2</sub>-ZrO<sub>2</sub> catalyst by potassium for  
4 NO<sub>x</sub>-assisted soot oxidation. *J. Envi. Sci.* **2011**, *23*, 145-150.  
5  
6
- 7 12. Weng, D.; Li, J.; Wu, X.; Si, Z. NO<sub>x</sub>-assisted soot oxidation over K/CuCe catalyst. *J.Rare*  
8  
9 *Earths.* **2010**, *28*, 542-546.  
10
- 11 13. Aneggi, E.; Boaro, M.; Leitenburg, C. d.; Dolcetti, G.; Trovarelli, A. Insights into the  
12 Redox Properties of Ceria-Based Oxides and Their Implications in Catalysis. *J. Alloy & Com.*  
13  
14 **2006**, *408-412*, 1096-1102.  
15  
16
- 17 14. Kai, L.; Xuezhong, W.; Zexing, Z.; Xiaodong, W.; Duan, W. Oxygen Storage Capacity of  
18 Pt-, Pd-, Rh/CeO<sub>2</sub>-Based Oxide Catalyst. *J. Rare Earths.* **2007**, *25*, 6-10.  
19  
20
- 21 15. Trovarelli, A. Catalytic Properties of Ceria and CeO<sub>2</sub>-Containing Materials. *Catal. Rev.*  
22  
23 **1996**, *38*, 439-520.  
24  
25
- 26 16. Epling, W. S.; Campbell, L. E.; Yezerets, A.; Currier, N. W.; Parks, J. E. Overview of the  
27 Fundamental Reactions and Degradation Mechanisms of NO<sub>x</sub> Storage/Reduction Catalysts.  
28  
29 *Catal.Rev.* **2004**, *46*, 163-245.  
30  
31
- 32 17. Hauff, K.; Tuttlies, U.; Eigenberger, G.; Nieken, U. Platinum Oxide Formation and  
33 Reduction during NO Oxidation on a Diesel Oxidation Catalyst-Experimental Results. *Appl.*  
34  
35 *Catal. B.* **2012**, *123-124*, 107-116.  
36  
37
- 38 18. Neyertz, C. A.; Miró, E. E.; Querini, C. A. K/CeO<sub>2</sub> Catalysts Supported on Cordierite  
39 Monoliths: Diesel Soot Combustion Study. *J. Chem. Eng.* **2012**, *81-182*, 93-102.  
40  
41
- 42 19. Konstandopoulos, A. G.; Papaioannou, E.; Zarvalis, D.; Skopa, S.; Baltzopoulou, P.;  
43 Kladopoulou, E.; Kostoglou, M.; Lorentzou, S. Catalytic Filter Systems with Direct and Indirect  
44  
45 Soot Oxidation Activity. *SAE Technical Paper Series.* **2005**, 2005-01-0670.  
46  
47
- 48 20. Renzullo, A.; Tarabocchia, A.; Villata, G.; Mescia, D.; Caroca, J. C.; Raimondi, A.;  
49 Russo, N.; Fino, D.; Saracco, G.; Specchia, V. DPF Supporting Nano-Structured Perovskite  
50  
51 Catalysts for NO<sub>x</sub> and Diesel Soot Emission Control in Commercial Vehicles. *SAE Technical*  
52  
53 *Paper Series.* **2007**, 2007-01-4173.  
54  
55  
56  
57  
58  
59  
60

- 1  
2  
3  
4  
5  
6  
7  
8  
9  
10  
11  
12  
13  
14  
15  
16  
17  
18  
19  
20  
21  
22  
23  
24  
25  
26  
27  
28  
29  
30  
31  
32  
33  
34  
35  
36  
37  
38  
39  
40  
41  
42  
43  
44  
45  
46  
47  
48  
49  
50  
51  
52  
53  
54  
55  
56  
57  
58  
59  
60
21. Grossale, A.; Nova, I.; Tronconi, E.; Chatterjee, D.; Weibel, M. The Chemistry of the NO/NO<sub>2</sub>-NH<sub>3</sub> “fast” SCR Reaction over Fe-ZSM5 Investigated by Transient Reaction Analysis *J.Catal.* **2008**, *256*, 312-322.
22. Luo, J.-Y.; Hou, X.; Wijayakoon, P.; Schmiegel, S. J.; Li, W.; Epling, W. S. Spatially Resolving SCR Reactions over a Fe/zeolite Catalyst. *Appl.Catal. B.* **2011**, *102*, 110-119.
23. Saidina Amin, N. A.; Chong, C. M. SCR of NO with C<sub>3</sub>H<sub>6</sub> in the Presence of Excess O<sub>2</sub> over Cu/Ag/CeO<sub>2</sub>-ZrO<sub>2</sub> Catalyst. *J. Chem. Eng.* **2005**, *113*, 13-25.
24. Kotsifa, A.; Kondarides, D. I.; Verykios, X. E. A Comparative Study of the Selective Catalytic Reduction of NO by Propylene over Supported Pt and Rh Catalysts. *Appl.Catal. B.* **2008**, *80*, 260-270.
25. Cant, N. W.; Angove, D. E.; Chambers, D. C. Nitrous Oxide Formation during the Reaction of Simulated Exhaust Streams over Rhodium, Platinum and Palladium Catalysts. *Appl. Catal. B.* **1998**, *17*, 63-73.
26. Qi, G.; Yang, R. T.; Chang, R. MnO<sub>x</sub>-CeO<sub>2</sub> Mixed Oxides Prepared by Co-Precipitation for Selective Catalytic Reduction of NO with NH<sub>3</sub> at Low Temperatures. *Appl. Catal. B.* **2004**, *51*, 93-106.
27. Gao, X.; Jiang, Y.; Zhong, Y.; Luo, Z.; Cen, K. The Activity and Characterization of CeO<sub>2</sub>-TiO<sub>2</sub> Catalysts Prepared by the Sol-Gel Method for Selective Catalytic Reduction of NO with NH<sub>3</sub>. *J. Hazardous Mater.* **2010**, *174*, 734-739.
28. Shan, W.; Liu, F.; He, H.; Shi, X.; Zhang, C. A Superior Ce-W-Ti Mixed Oxide Catalyst for the Selective Catalytic Reduction of NO<sub>x</sub> with NH<sub>3</sub>. *Appl. Catal. B.* **2012**, *115-116*, 100-106.
29. Long, R. Q.; Yang, R. T. The Promoting Role of Rare Earth Oxides on Fe-Exchanged TiO<sub>2</sub>-Pillared Clay for Selective Catalytic Reduction of Nitric Oxide by Ammonia. *Appl. Catal. B.* **2000**, *27*, 87-95.
30. Qi, G.; Yang, R. T. Performance and Kinetics Study for Low-Temperature SCR of NO with NH<sub>3</sub> over MnO<sub>x</sub>-CeO<sub>2</sub> Catalyst. *J. Catal.* **2003**, *217*, 434-441.

- 1  
2  
3  
4  
5  
6  
7  
8  
9  
10  
11  
12  
13  
14  
15  
16  
17  
18  
19  
20  
21  
22  
23  
24  
25  
26  
27  
28  
29  
30  
31  
32  
33  
34  
35  
36  
37  
38  
39  
40  
41  
42  
43  
44  
45  
46  
47  
48  
49  
50  
51  
52  
53  
54  
55  
56  
57  
58  
59  
60
31. Zhang, L.; Liu, F.; Yu, Y.; Liu, Y.; Zhang, C.; He, H. Effects of Adding CeO<sub>2</sub> to Ag/Al<sub>2</sub>O<sub>3</sub> Catalyst for Ammonia Oxidation at Low Temperatures. *Chin. J. Catal.* **2011**, *32*, 727-735.
32. Setiabudi, A.; Makkee, M.; Moulijn, J. A. The Role of NO<sub>2</sub> and O<sub>2</sub> in the Accelerated Combustion of Soot in Diesel Exhaust Gases. *Appl. Catal. B.* **2004**, *50*, 185-194.
33. Liu, S.; Obuchi, A.; Uchisawa, J.; Nanba, T.; Kushiyama, S. An Exploratory Study of Diesel Soot Oxidation with NO<sub>2</sub> and O<sub>2</sub> on Supported Metal Oxide Catalysts. *Appl. Catal. B.* **2002**, *37*, 309-319.
34. Shen, B.; Liu, T.; Zhao, N.; Yang, X.; Deng, L. Iron-Doped Mn-Ce/TiO<sub>2</sub> Catalyst for Low Temperature Selective Catalytic Reduction of NO with NH<sub>3</sub>. *J. Envi. Sci.* **2010**, *22*, 1447-1454.
35. Burch, R.; Breen, J. P.; Meunier, F. C. A Review of the Selective Reduction of NO<sub>x</sub> with Hydrocarbons under Lean-Burn Conditions with Non-Zeolitic Oxide and Platinum Group Metal Catalysts. *Appl. Catal. B.* **2002**, *39*, 283-303.
36. Zhang, L.; He, H. Mechanism of Selective Catalytic Oxidation of Ammonia to Nitrogen over Ag/Al<sub>2</sub>O<sub>3</sub>. *J. Catal.* **2009**, *268*, 18-25.
37. Lin, S. D.; Gluhoi, A. C.; Nieuwenhuys, B. E. Ammonia Oxidation over Au/MO<sub>x</sub>/□ - Al<sub>2</sub>O<sub>3</sub>-Activity, Selectivity and FTIR Measurements. *Catal. Today.* **2004**, *90*, 3-14.
38. Amores, J. G.; Escribano, V. S.; Ramis, G.; Busca, G. An FT-IR Study of Ammonia Adsorption and Oxidation over Anatase-Supported Metal Oxides. *Appl. Catal. B.* **1997**, *13*, 45-58.
39. Toops, T. J.; Smith, D. B.; Epling, W. S.; Parks, J. E.; Partridge, W. P. Quantified NO<sub>x</sub> Adsorption on Pt/K/Gamma-Al<sub>2</sub>O<sub>3</sub> and the Effects of CO<sub>2</sub> and H<sub>2</sub>O. *Appl. Catal. B.* **2005**, *58*, 255-264.
40. Kantcheva, M. Identification, Stability, and Reactivity of NO<sub>x</sub> Species Adsorbed on Titania-Supported Manganese Catalysts. *J. Catal.* **2001**, *204*, 479-494.

- 1  
2  
3 41. Westerberg, B.; Fridell, E. A Transient FTIR Study of Species Formed during NO<sub>x</sub>  
4 Storage in the Pt/BaO/Al<sub>2</sub>O<sub>3</sub> System. *J. Molec. Catal. A.* **2001**, *165*, 249-263.  
5  
6  
7 42. Chen, L.; Li, J.; Ge, M.; Ma, L.; Chang, H. Mechanism of Selective Catalytic Reduction  
8 of NO<sub>x</sub> with NH<sub>3</sub> over CeO<sub>2</sub>-WO<sub>3</sub> Catalysts. *Chin. J. Catal.* **2011**, *32*, 836-841.  
9  
10 43. Nolan, M.; Parker, S. C.; Watson, G. W. Reduction of NO<sub>2</sub> on Ceria Surfaces. *J. Phy.*  
11 *Chem.B* **2006**, *110*, 2256-2262.  
12  
13  
14  
15  
16  
17  
18  
19  
20  
21  
22  
23  
24  
25  
26  
27  
28  
29  
30  
31  
32  
33  
34  
35  
36  
37  
38  
39  
40  
41  
42  
43  
44  
45  
46  
47  
48  
49  
50  
51  
52  
53  
54  
55  
56  
57  
58  
59  
60

**Figure captions**

**Figure 1.** NH<sub>3</sub> and NO conversion over fully oxidized CeO<sub>2</sub>. Reaction conditions: 500 ppm NH<sub>3</sub>, 500 ppm NO, 10% O<sub>2</sub> and balance N<sub>2</sub> with a total flow rate of 200 cm<sup>3</sup>·min<sup>-1</sup> (GHSV = 18,000 h<sup>-1</sup>).

**Figure 2.** NH<sub>3</sub> conversion and products selectivity over fully oxidized CeO<sub>2</sub>. Reaction conditions: 500 ppm NH<sub>3</sub>, 10% O<sub>2</sub> and balance N<sub>2</sub> with a total flow rate of 200 cm<sup>3</sup>·min<sup>-1</sup> (GHSV = 18,000 h<sup>-1</sup>).

**Figure 3.** Reactor outlet (a) NH<sub>3</sub>, (b) NO and (c) N<sub>2</sub>O concentration profiles upon exposure of 1.0 g fully oxidized ceria to 500 ppm NH<sub>3</sub> and balance N<sub>2</sub>.

**Figure 4.** NO<sub>2</sub> formed during NO oxidation over ceria. Reaction conditions: 500 ppm NO, 5% O<sub>2</sub> and balance N<sub>2</sub> balance with a total flow rate of 200 cm<sup>3</sup>·min<sup>-1</sup> (GHSV = 18,000 h<sup>-1</sup>).

**Figure 5.** Reactor outlet (a) NO and (b) NO<sub>2</sub> concentration profiles upon exposure of the fully oxidized ceria to 500 ppm NO and balance N<sub>2</sub>.

**Figure 6.** DRIFTS spectra obtained during exposure of the (a) fully oxidized and (b) reduced CeO<sub>2</sub> to 500 ppm NH<sub>3</sub> and balance He at room temperature and then the temperature changed in only a He flow; with a total flow rate of 50 cm<sup>3</sup>·min<sup>-1</sup>.

**Figure 7.** DRIFTS spectra obtained during exposure of the (a) fully oxidized and (b) reduced CeO<sub>2</sub> to 500 ppm NO and balance He at room temperature and then the temperature changed in only a He flow; with a total flow rate of 50 cm<sup>3</sup>·min<sup>-1</sup>.

**Figure 8.** DRIFTS spectra obtained during exposure of the reduced CeO<sub>2</sub> to 500 ppm NO<sub>2</sub> and balance He at room temperature and then the temperature changed in only a He flow; with a total flow rate of 50 cm<sup>3</sup>·min<sup>-1</sup>.

**Figure 9.** DRIFTS spectra obtained during exposure of the fully oxidized ceria to (a) 500 ppm NH<sub>3</sub> + 10% O<sub>2</sub> and (b) 500 ppm NH<sub>3</sub> + 500 ppm NO + 10 % O<sub>2</sub> with He as the balance with a total flow rate of 50 cm<sup>3</sup>·min<sup>-1</sup>.

1  
2  
3 **Figure 10.** DRIFTS spectra obtained during exposure of the fully oxidized ceria to NH<sub>3</sub>  
4 after pre-adsorption of (a) NO and (b) NO<sub>2</sub> at 350°C. Reaction conditions: 500 ppm NO  
5 or NO<sub>2</sub> adsorbed over the sample at 350°C and then purged by He followed by exposure  
6 to 500 ppm NH<sub>3</sub> with a total flow rate of 50 cm<sup>3</sup>·min<sup>-1</sup>.  
7  
8  
9  
10  
11  
12  
13  
14  
15  
16  
17  
18  
19  
20  
21  
22  
23  
24  
25  
26  
27  
28  
29  
30  
31  
32  
33  
34  
35  
36  
37  
38  
39  
40  
41  
42  
43  
44  
45  
46  
47  
48  
49  
50  
51  
52  
53  
54  
55  
56  
57  
58  
59  
60

1  
2  
3 **Table 1.** NH<sub>3</sub> consumed and NO and N<sub>2</sub>O formed during NO interaction with fully oxidized ceria  
4  
5  
6 at different temperatures.  
7

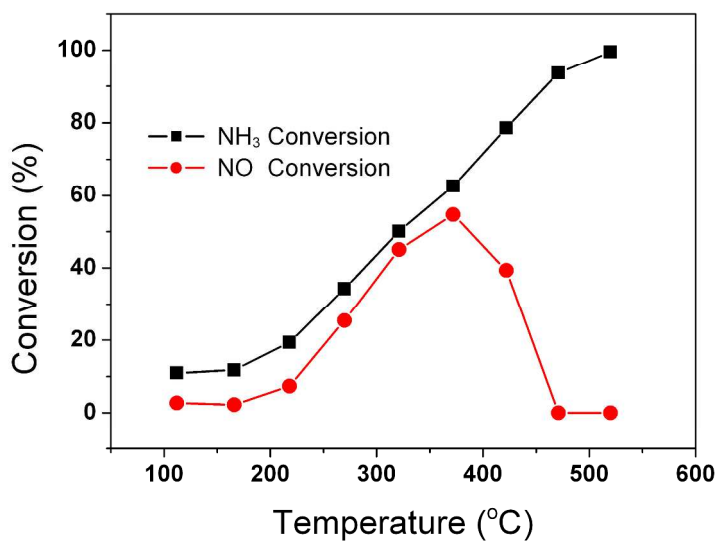
8  
9  
10  
11  
12  
13  
14  
15  
16  
17  
18  
19

Temperature (°C)	NO formed (μmol)	N <sub>2</sub> O formed (μmol)	NH <sub>3</sub> Consumed (μmol)
350	4.5	1.2	26.0
400	14.6	2.8	38.8
450	20.9	1.6	50.4

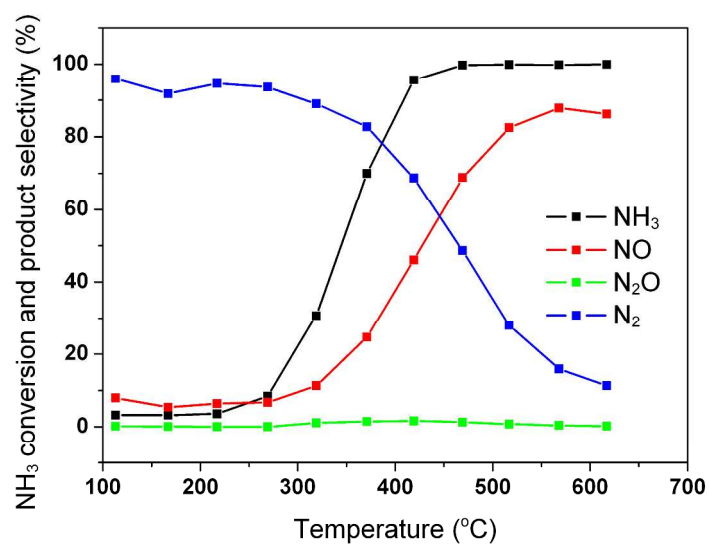
20  
21  
22 **Table 2.** Surface oxygen uptake by NO and the adsorbed nitrates on the surface of ceria at  
23  
24 various temperatures during the transient NO interaction with fully oxidized ceria at different  
25  
26 temperatures.  
27  
28  
29

30  
31  
32  
33  
34  
35  
36  
37  
38  
39  
40  
41  
42  
43  
44  
45  
46  
47  
48  
49  
50  
51  
52  
53  
54  
55  
56  
57  
58  
59  
60

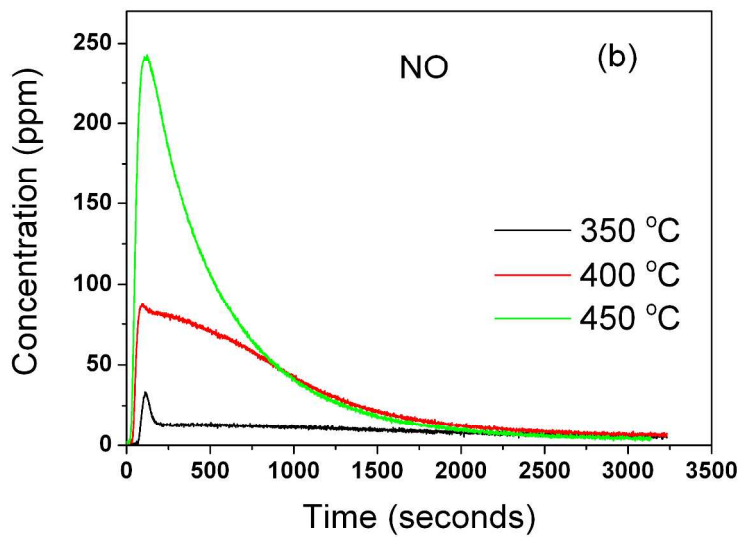
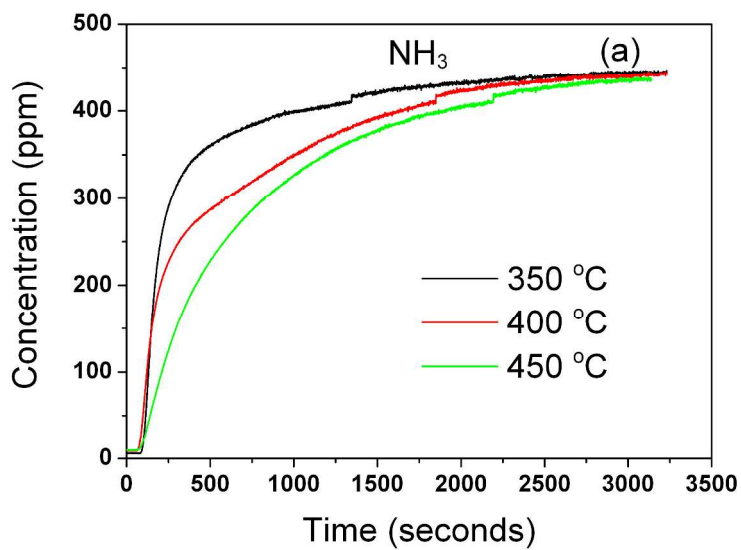
Temperature (°C)	O <sub>s</sub> (μmol)	Nitrates (μmol)
30	664	664
100	1991	1991
150	1580	1580
200	1033	1033
250	640	640
300	363	363
350	318	318
400	292	288
450	268	266
500	223	219



**Figure 1.** NH<sub>3</sub> and NO conversion over fully oxidized CeO<sub>2</sub>. Reaction conditions: 500 ppm NH<sub>3</sub>, 500 ppm NO, 10% O<sub>2</sub> and balance N<sub>2</sub> with a total flow rate of 200 cm<sup>3</sup>·min<sup>-1</sup> (GHSV = 18,000 h<sup>-1</sup>).



**Figure 2.** NH<sub>3</sub> conversion and products selectivity over fully oxidized CeO<sub>2</sub>. Reaction conditions: 500 ppm NH<sub>3</sub>, 10% O<sub>2</sub> and balance N<sub>2</sub> with a total flow rate of 200 cm<sup>3</sup>·min<sup>-1</sup> (GHSV = 18,000 h<sup>-1</sup>).



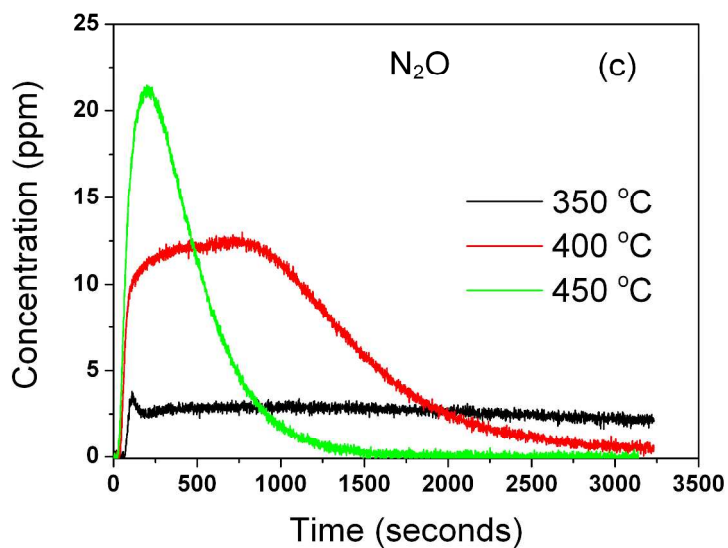


**Figure 3.** Reactor outlet (a) NH<sub>3</sub>, (b) NO and (c) N<sub>2</sub>O concentration profiles upon exposure of 1.0 g fully oxidized ceria to 500 ppm NH<sub>3</sub> and balance N<sub>2</sub>.

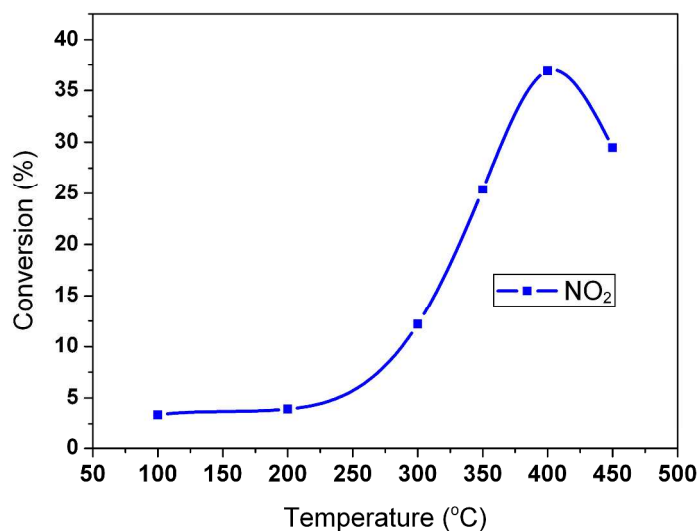


**Figure 4.** NO<sub>2</sub> formed during NO oxidation over ceria. Reaction conditions: 500 ppm NO, 5% O<sub>2</sub> and balance N<sub>2</sub> balance with a total flow rate of 200 cm<sup>3</sup>·min<sup>-1</sup> (GHSV = 18,000 h<sup>-1</sup>).

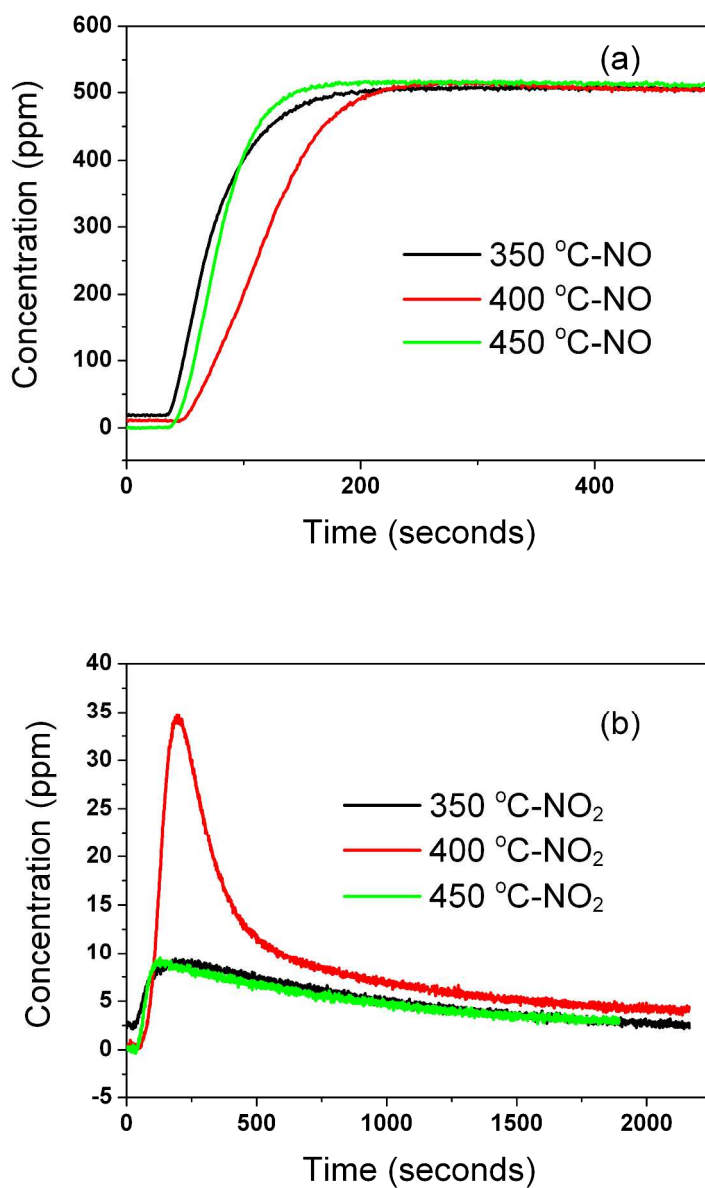


**Figure 5.** Reactor outlet (a) NO and (b) NO<sub>2</sub> concentration profiles upon exposure of the fully oxidized ceria to 500 ppm NO and balance N<sub>2</sub>.

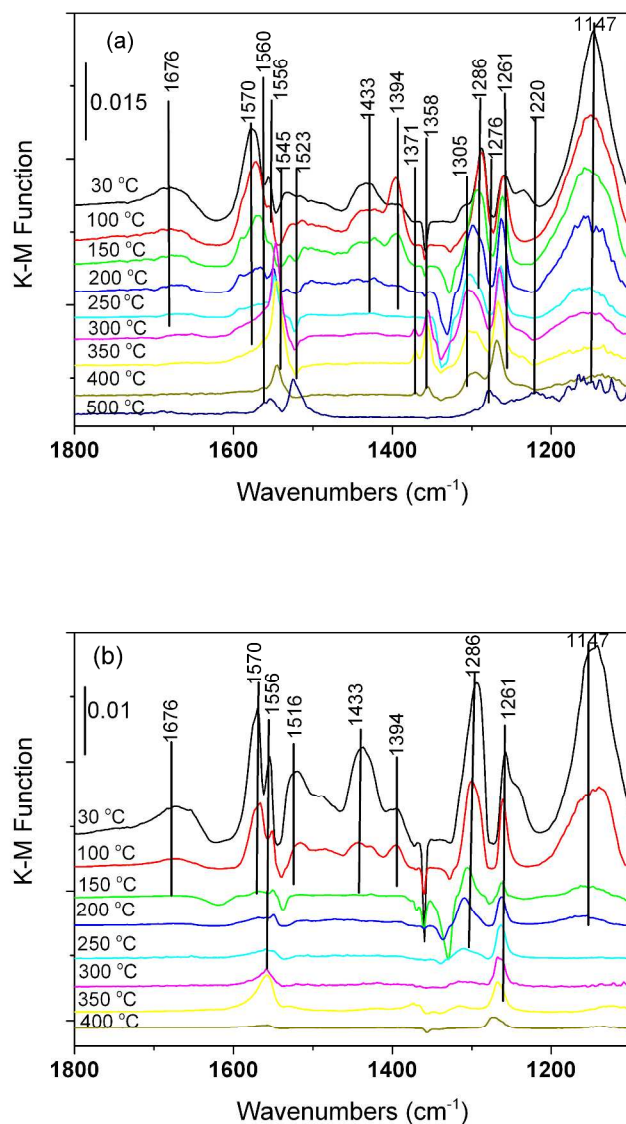


**Figure 6.** DRIFTS spectra obtained during exposure of the (a) fully oxidized and (b) reduced CeO<sub>2</sub> to 500 ppm NH<sub>3</sub> and balance He at room temperature and then the temperature changed in only a He flow; with a total flow rate of 50 cm<sup>3</sup>·min<sup>-1</sup>.

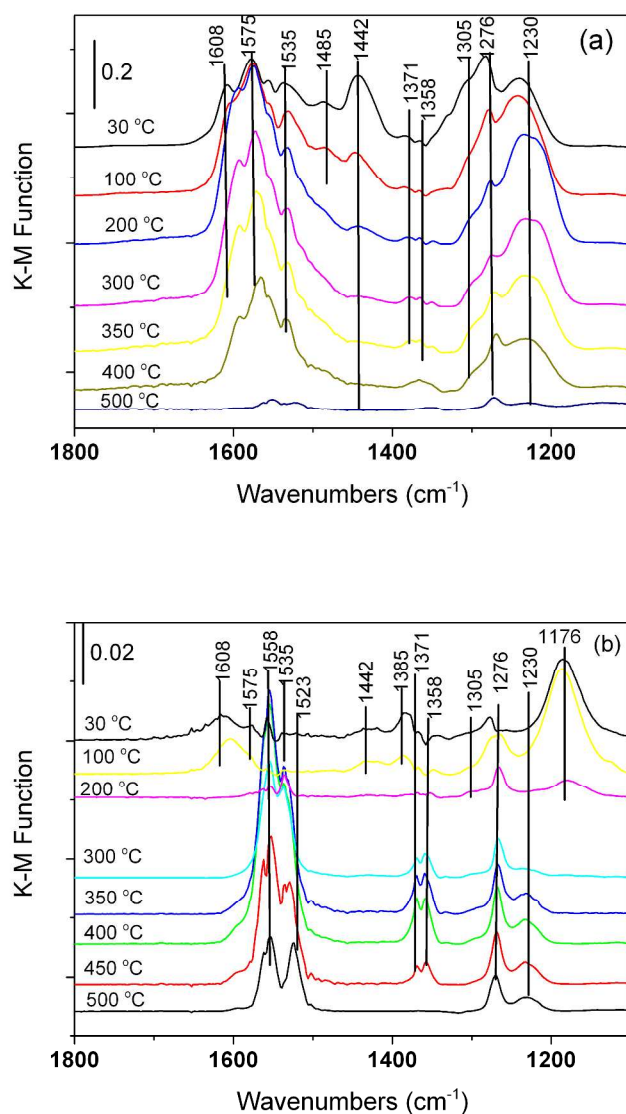


**Figure 7.** DRIFTS spectra obtained during exposure of the (a) fully oxidized and (b) reduced CeO<sub>2</sub> to 500 ppm NO and balance He at room temperature and then the temperature changed in only a He flow; with a total flow rate of 50 cm<sup>3</sup>·min<sup>-1</sup>.

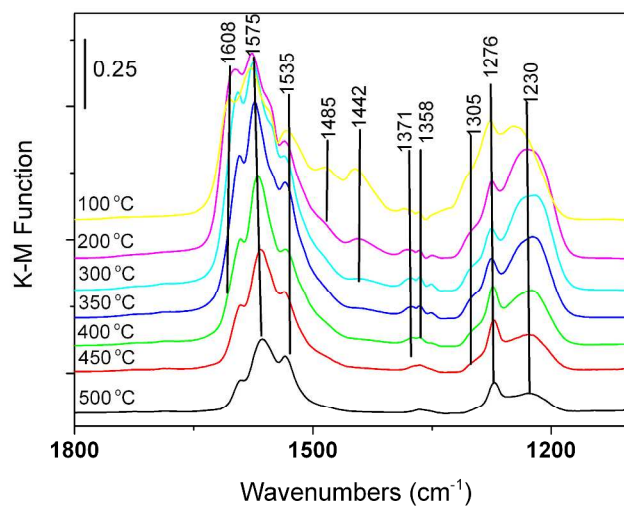


**Figure 8.** DRIFTS spectra obtained during exposure of the reduced CeO<sub>2</sub> to 500 ppm NO<sub>2</sub> and balance He at room temperature and then the temperature changed in only a He flow; with a total flow rate of 50 cm<sup>3</sup>·min<sup>-1</sup>.

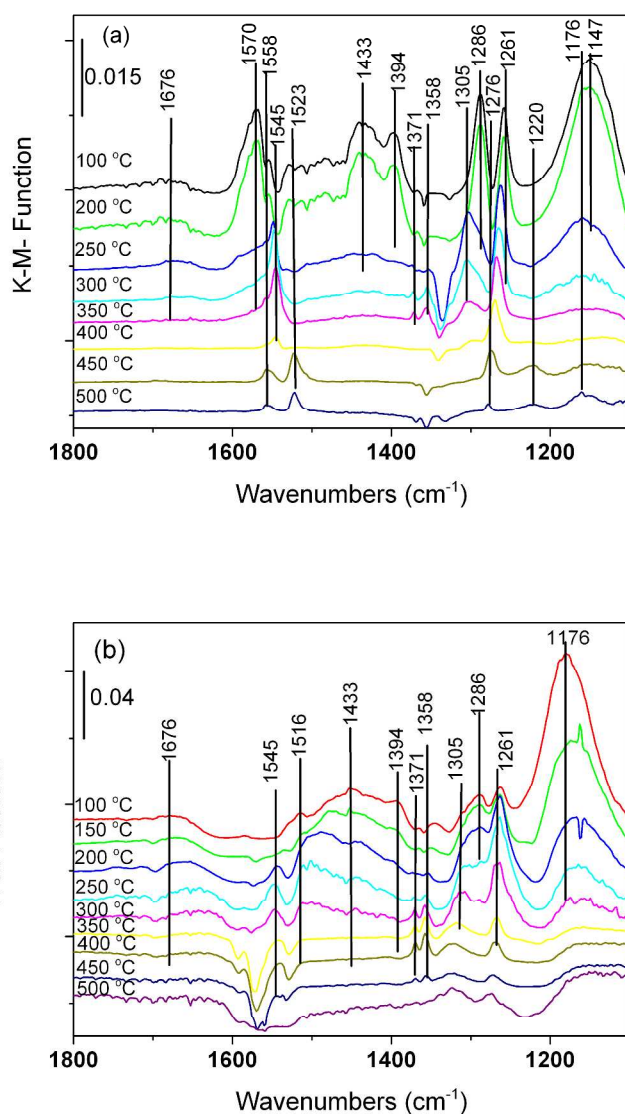


**Figure 9.** DRIFTS spectra obtained during exposure of the fully oxidized ceria to (a) 500 ppm NH<sub>3</sub> + 10% O<sub>2</sub> and (b) 500 ppm NH<sub>3</sub> + 500 ppm NO + 10 % O<sub>2</sub> with He as the balance with a total flow rate of 50 cm<sup>3</sup>·min<sup>-1</sup>.

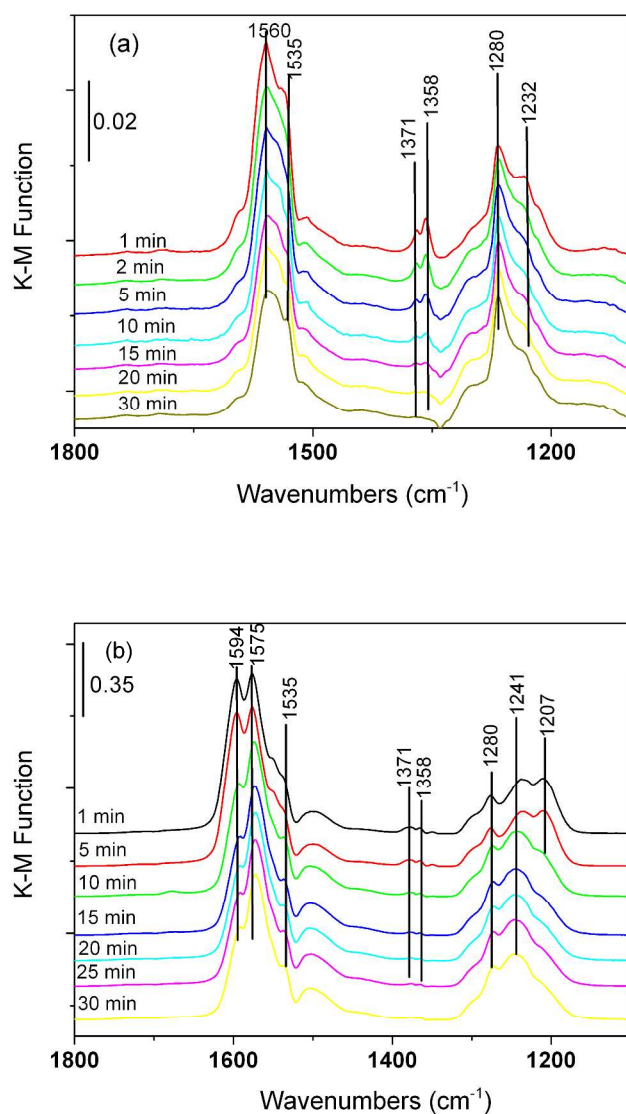


**Figure 10.** DRIFTS spectra obtained during exposure of the fully oxidized ceria to NH<sub>3</sub> after pre-adsorption of (a) NO and (b) NO<sub>2</sub> at 350°C. Reaction conditions: 500 ppm NO or NO<sub>2</sub> adsorbed over the sample at 350°C and then purged by He followed by exposure to 500 ppm NH<sub>3</sub> with a total flow rate of 50 cm<sup>3</sup>·min<sup>-1</sup>.

TOC Figure

